NASA
Technical
Paper
2746

July 1987

Low-Cost FM Oscillator for Capacitance Type of Blade Tip Clearance Measurement System

John P. Barranger

NASA

NASA
Technical
Paper
2746

1987

Low-Cost FM Oscillator for Capacitance Type of Blade Tip Clearance Measurement System

John P. Barranger

Lewis Research Center
Cleveland, Ohio

National Aeronautics
and Space Administration

**Scientific and Technical
Information Office**

Trade names or manufacturers' names are used in this report for identification only. The usage does not constitute an official endorsement, either expressed or implied, by the National Aeronautics and Space Administration.

Summary

The frequency-modulated (FM) oscillator described in this report is part of a blade tip clearance measurement system that meets the needs of a wide class of fans, compressors, and turbines. As a result of advancements in the technology of ultra-high-frequency operational amplifiers, the FM oscillator requires only a single low-cost integrated circuit. Its carrier frequency is 42.8 MHz when it is used with an integrated probe and connecting cable assembly consisting of a 0.81-cm (0.32-in.) diameter engine-mounted capacitance probe and a 61-cm (24-in.) long hermetically sealed coaxial cable. A complete circuit analysis is given, including amplifier negative resistance characteristics. An error analysis of environmentally induced effects is also derived, and an error-correcting technique is proposed. The oscillator can be calibrated in the static mode and has a negative peak frequency deviation of 400 kHz for a rotor blade thickness of 1.2 mm (0.047 in.). High-temperature performance tests of the probe and 13 cm (5 in.) of the adjacent cable show good accuracy up to 600 °C (1110 °F), the maximum permissible seal temperature. The major source of error is the residual FM oscillator noise, which produces a clearance error of ± 10 μm (± 0.4 mil) at a clearance of 0.5 mm (0.02 in.). The oscillator electronics accommodates the high rotor speeds associated with small engines, the signals from which may have frequency components as high as 1 MHz.

Introduction

The need for blade tip clearance instrumentation has been intensified recently by advances in the technology of gas turbine engines. Improved engine designs encompass light-weight high-performance concepts such as small, thin airfoils for blades. Excess blade tip clearance allows a portion of the engine gas to flow over the blade tip without performing useful work. Moreover, insufficient clearance may cause interference that can jeopardize engine integrity.

Measurement of blade tip clearance is important to the design, development, and operation of fans, compressors, and turbines. During the design phase computational codes are generated to predict engine behavior under operational conditions. Verification of these codes requires comparing predicted values with experimental measurements. Full development mandates monitoring of blade tip clearances over the entire flight envelope. Finally, maximum engine efficiency during operational flight can only be achieved through active control of blade tip clearance.

Capacitance sensors are applied extensively to the measurement of blade tip clearance. The most widely used techniques are impedance voltage division (ref. 1), feedback operational amplification (ref. 2), frequency-modulated (FM) oscillation (refs. 3 and 4), phase shifting (refs. 5 and 6), Coulomb-charge conversion (ref. 7), and others (refs. 8 and 9). A recent technique is ramp integration (ref. 10).

The FM oscillator described in this report is part of a blade tip clearance measurement system that meets the needs of a wide class of gas turbine engines. Its carrier frequency is 42.8 MHz when it is used with an integrated probe and connecting cable assembly consisting of a 0.81-cm (0.32-in.) diameter engine-mounted capacitance probe and a 61-cm (24-in.) long hermetically sealed coaxial cable. A complete circuit analysis is given, including amplifier negative resistance characteristics. An error analysis of environmentally induced effects is also derived, and an error-correcting technique is proposed. The oscillator can be calibrated in the static mode and has a negative peak frequency deviation of 400 kHz for a rotor blade thickness of 1.2 mm (0.047 in.). High-temperature performance tests of the probe and 13 cm (5 in.) of the adjacent cable show good accuracy up to 600 °C (1110 °F), the maximum permissible seal temperature. The major source of error is the residual FM oscillator noise, which produces a clearance error of ± 10 μm (± 0.4 mil) at a clearance of 0.5 mm (0.02 in.). The oscillator accommodates the high rotor speeds associated with small engines, the signals from which may have frequency components as high as 1 MHz.

As a result of advancements in the technology of ultra-high-frequency operational amplifiers, the FM oscillator requires only a single low-cost integrated circuit. This simplification yields high economic gains for multiprobe systems. Moreover, miniature wideband frequency demodulators (discriminators) are now commercially available to process the output of the oscillator.

Some important advantages over other FM oscillator designs result from the use of a carrier frequency within the range 30 to 50 MHz. A carrier frequency of less the 50 MHz allows the connecting cable to be at least twice as long as for designs at 100 MHz (ref. 3). This is critical for high-temperature applications, where greater physical separation is required between the probe and the oscillator electronics. Furthermore

output filters for the discriminator have greater attenuation at carrier frequencies above 30 MHz than in the 1- to 10-MHz range (ref. 4).

System Description and Environmental Considerations

The clearance measurement system (fig. 1) consists of an electronics unit, a coaxial connecting cable, and a capacitance probe. The electronics unit contains the FM oscillator electronics and the signal conditioner. The signal conditioner demodulates the oscillator output and provides a signal suitable for the data acquisition unit. Neither the signal conditioner nor the data acquisition unit will be discussed.

In the capacitance probe installation (fig. 2) the clearance d is defined as the distance between the rotor blade tip and the shroud. This is also the distance to the probe face since the probe is mounted flush with the shroud. (In some engines the shroud has an abradable inner liner that wears away by blade rubbing action. This situation was not considered in the present probe design, but a probe tip made of abradable materials that wears away with the liner is a possible solution.)

Terminal pair 1-1′ (fig. 2) represents the connection between the end of the coaxial cable and the probe. The probe has coaxial construction, where the inner conductor is separated from the outer tube by an insulator. As shown in the figure the inner conductor can be in the form of a solid round rod or a wire terminated in a disk.

The capacitance looking into terminal pair 1-1′ can be thought of as the sum of the capacitance of the probe alone and the capacitance introduced by the presence of the blade. To visualize this concept, imagine that two blades with different clearances pass under the probe. The total capacitance for the two blades as a function of time t would be $C(t)$, as shown in figure 3. Making the probe diameter much smaller than the interblade spacing results in $C(t)$ becoming equal to the capacitance of the probe alone between blade pairs. Let this probe capacitance be called C_o. At the point of maximum capacitance

$$C_m = C_o + C(d) \tag{1}$$

where $C(d)$ is the blade capacitance and d is the clearance between the blade tip and the probe face. The value of $C(d)$ increases as d decreases and is usually very small, typically 1 pF or less.

Environmental conditions affect all components of the system. The probe, which is subject to the most severe environment, can be characterized by its geometry and the electrical properties and characteristics of the insulator. It is known that the electrical properties of insulator materials change with temperature and that the characteristics of exposed insulator surfaces are subject to changes in humidity.

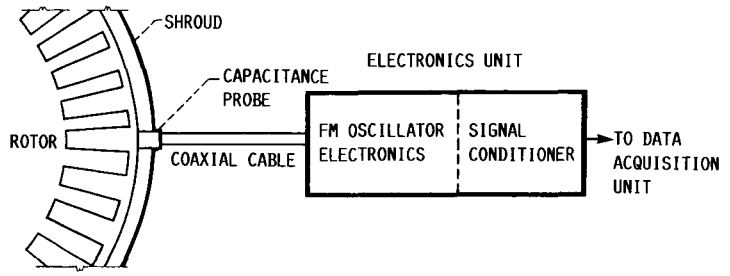

Figure 1.—Block diagram of blade tip clearance measurement system.

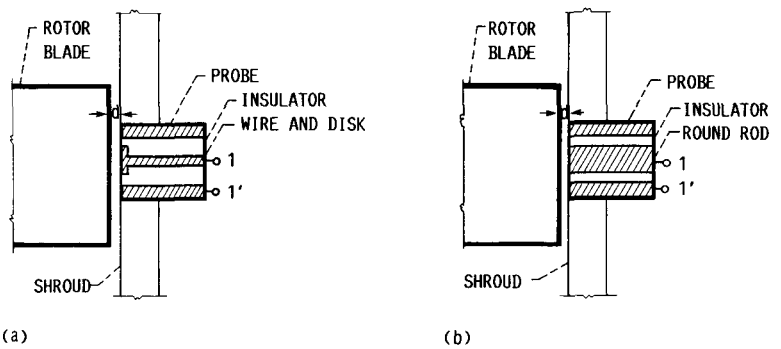

(a) Wire-and-disk inner conductor.
(b) Round-rod inner conductor.

Figure 2.—Schematic of capacitance probe installation.

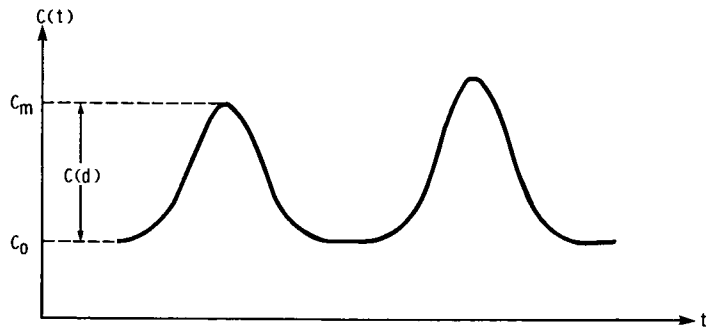

Figure 3.—Capacitance as function of time for two blades to pass under probe tip.

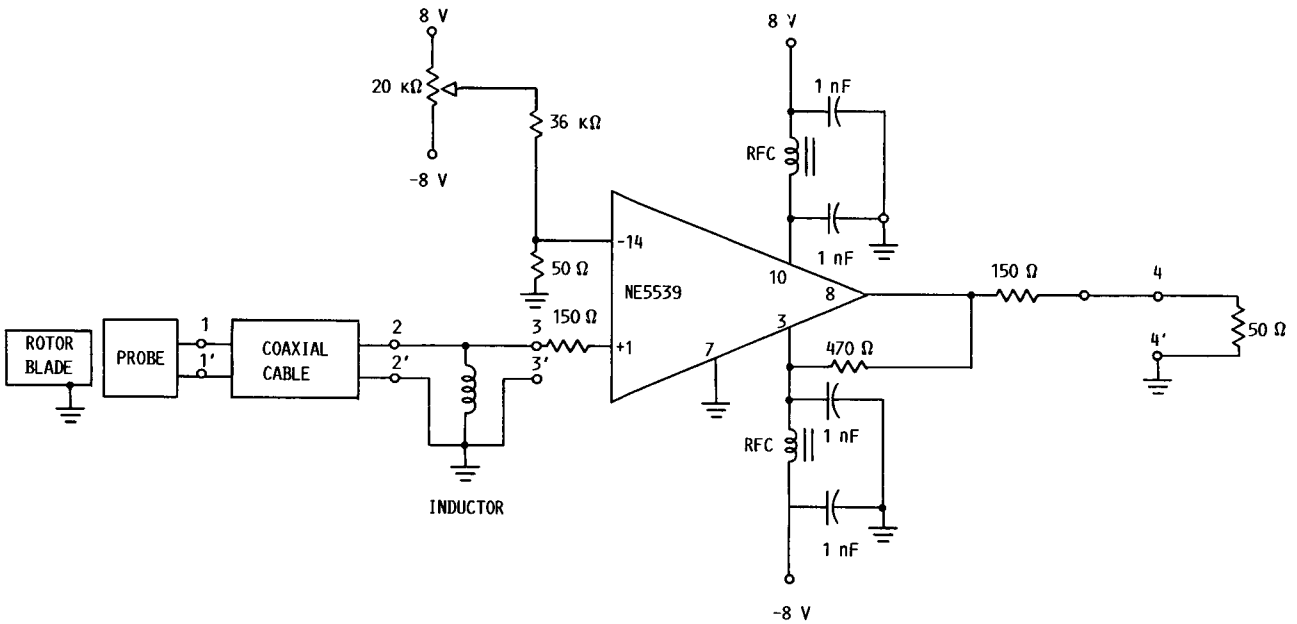

Figure 4.—Schematic of FM oscillator. Inductor: 0.17 to 0.27 μH, adjustable (Miller 4301); radiofrequency choke (RFC): three turns of no. 26 bus wire on Ferroxcube VK 200 09/3B core.

Furthermore, if the probe is in the turbine section of the engine, the insulator surface may become contaminated by combustion products such as soot and metal particles. Thus the probe is affected by temperature, humidity, and engine-generated contamination.

Some of the environmental conditions that influence the probe also affect the coaxial cable connecting the probe to the electronics unit. The insulator material properties change with temperature and cause variations in the cable's transmission line parameters. Being more flexible than the rigid probe, the cable is also subject to engine-induced mechanical vibration.

Because of the high frequency of the FM oscillator the electronics unit is placed close to the engine. Therefore a means must be provided to keep its temperature under the maximum operating temperature of its components. The electronics unit must also be vibration and acoustically isolated, and due consideration must be given to the mechanical layout of the circuits.

The most critical part of the electronics is the means used to convert the changes in capacitance caused by a passing blade to an electrical signal that can ultimately be processed to yield the clearance. The electrical circuit for that means is described and analyzed in the following section.

FM Oscillator

Circuit Description

The probe and the coaxial cable are an integrated assembly in the FM oscillator (fig. 4). A wire terminating in a disk, as illustrated in figure 2(a), is the probe inner conductor. The probe is 0.81 cm (0.32 in.) in outside diameter and 1.5 cm (0.59 in.) long. The disk is 4.4 mm (0.17 in.) in diameter. The probe insulator is ceramic and is set back 0.64 cm (0.25 in.) from the probe face. The cable portion of the assembly is a high-temperature "semirigid" coaxial cable

consisting of a stainless-steel-clad copper outer conductor and a solid copper inner conductor separated by a silica dielectric. End seals maintain hermetic integrity up to 600 °C (1110 °F). The characteristic impedance of the cable is 50 Ω, and its distributed capacitance is 82 pF/m (25 pF/ft). The cable is 3.61 mm (0.142 in.) in outside diameter and 61 cm (24 in.) long. Connection to the FM oscillator electronics is made via an SMA type of radiofrequency (RF) connector.

The NE5539 (fig. 4) is a low-cost, ultra-high-frequency operational amplifier fabricated in a monolithic, 14-pin integrated-circuit package. Electrical resonance is achieved by the network consisting of the inductor and its effective parallel capacitance, of which the blade capacitance is a part. Since there is no explicit feedback from the output of the amplifier, this kind of circuit is usually called a two-terminal negative resistance oscillator.

A 50-Ω resistor loads the output of the oscillator circuit across terminal pair 4-4′ (fig. 4). The load can be the input impedance of the next stage or of a transmission line carrying the oscillator output to a remote location. Thus the operational amplifier acts as both an oscillator active element and a line driver.

Figure 5 is the equivalent electrical network of the components of figure 4 that characterize the oscillator. Each of these elements is a model of the component in the frequency range of interest. Probe admittance Y_1 is the parallel combination of the reactance of the total capacitance C and the conductance G_o. The admittance looking into the coaxial cable terminal pair 2-2′ loaded by Y_1 at terminal pair 1-1′ is Y_2. The coaxial cable is considered to be the parallel combination of a lumped shunt capacitance C_T and a lumped shunt conductance G_T. Appendix A develops this equivalent network of the coaxial cable based on a short, lightly loaded nonideal transmission line subject to high temperatures.

The inductor is approximated by an equivalent network consisting of an inductance L in series with a resistance R and a shunt capacitance C_L. As with most RF inductors the ratio of its inductive reactance to its series resistance, or Q, is much larger than unity in the frequency range of interest. Shunt capacitance accounts for the parallel self-resonance of the inductor at very high frequencies. The resonant frequency of the oscillator must be less than the self-resonant frequency of the inductor.

Capacitance C_k is the total shunt circuit capacitance, which includes both the connector and wiring capacitances.

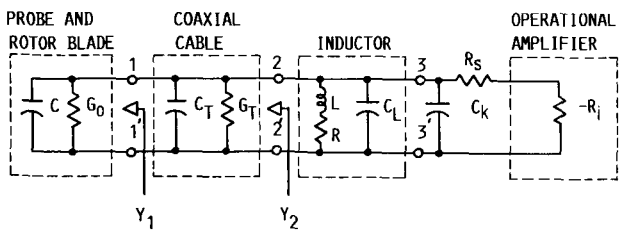

Figure 5.—Equivalent network of components in figure 4 that characterize oscillator.

Resistance R_s is in series with the positive input terminal of the operational amplifier.

All oscillators require an active element that simulates negative resistance. In this case the operational amplifier generates this negative resistance plus some incidental reactance between the positive input terminal and ground. As shown in the subsection "Calibration and Circuit Measurements" the effect of this reactance is small and can therefore be neglected. The input impedance of the amplifier is then simply the negative resistance, designated $-R_i$.

Circuit Analysis

An important aspect of FM oscillator design is the choice of the oscillating frequency. To apply the equivalent network described in appendix A, the electrical length of the coaxial cable must be less than one-fourth of the wavelength at this frequency. Thus lower frequencies permit longer connecting cables. This is critical for high-temperature applications, where greater physical separation is required between the probe and the oscillator electronics. On the other hand, discriminator output filter design is simplified at higher frequencies because of the greater attenuation.

The oscillation frequency is found by network analysis. Moreover an important consideration of any oscillator is the criteria under which the oscillation amplitude increases and reaches its steady state after initiation by noise. Analysis of the circuit will also yield this information.

In the following analysis linear models are assumed for all circuit elements. To reduce the number of factors in the equations, like elements in figure 5 have been combined, resulting in the reduced equivalent network of figure 6(a), where

$$C_p' = C + C_T + C_L + C_k \tag{2}$$

$$R_p = \frac{1}{G_o + G_T} \tag{3}$$

$$-R_i' = R_s - R_i \tag{4}$$

and L and R are unchanged. The quantity $-R_i'$ is the resistance looking toward the operational amplifier across terminal pair 3-3′ (fig. 5).

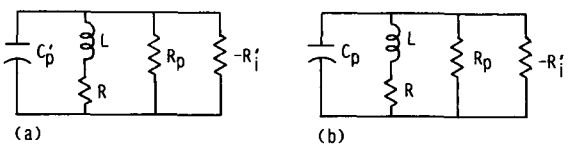

(a) $C_p' = C + C_T + C_L + C_k$.
(b) $C_p = C_o + C_T + C_L + C_k$.

Figure 6.—Reduced equivalent networks of figure 5.

Following the usual techniques for analyzing oscillator networks, let the presence of thermal noise produce voltages and currents of the form

$$\epsilon^{-\alpha t} \cos (2\pi f_d t + \theta) \tag{5}$$

where

$$f_d = \frac{1}{2\pi} \left[\frac{1 + R\left(\frac{1}{R_p} - \frac{1}{R_i'}\right)}{LC_p'} - \alpha^2 \right]^{1/2} > 0 \tag{6}$$

$$\alpha = \frac{1}{2C_p'}\left(\frac{RC_p'}{L} + \frac{1}{R_p} - \frac{1}{R_i'}\right) \tag{7}$$

and θ is the phase angle. It is clear that as long as the inequality

$$\frac{RC_p'}{L} + \frac{1}{R_p} - \frac{1}{R_i'} < 0 \tag{8}$$

is met, the oscillations will continue to increase in amplitude. It is equally clear that for a steady-state equilibrium condition, it is necessary that

$$\frac{RC_p'}{L} + \frac{1}{R_p} - \frac{1}{R_i'} = 0 \tag{9}$$

Thus $1/R_i'$ and therefore $1/R_i$ must be some function of amplitude. Specifically $1/R_i$ must decrease with amplitude until equation (9) is satisfied. This is the criterion under which the oscillation amplitude increases and reaches a steady state after initiation by noise. Included in appendix B is a plot illustrating the amplitude characteristic of a modified form of the left side of equations (8) and (9).

The oscillation frequency, under steady-state conditions is found by setting α in equation (6) to zero. Solving equations (6) and (9) simultaneously yields the formula

$$f_o = \frac{1}{2\pi}\left(\frac{1}{LC_p'}\right)^{1/2} \tag{10}$$

where

$$\frac{R^2 C_p'}{L} << 1 \tag{11}$$

for the resonant frequency f_o. Inequality (11) is valid for high-Q inductors used in oscillators of moderate accuracy. The resonant frequency when the probe is between blade pairs, that is, when $C = C_o$, is defined as the carrier frequency f_c. Thus

$$f_c = \frac{1}{2\pi}\left(\frac{1}{LC_p}\right)^{1/2} \tag{12}$$

where

$$C_p = C_o + C_T + C_L + C_k \tag{13}$$

The resultant equivalent network is shown in figure 6(b).

The blade passing under the probe causes a small change in the carrier frequency, defined as the frequency deviation. The maximum carrier frequency change, defined as the peak frequency deviation Δf_c, is found from

$$\Delta f_c = -\frac{C(d)}{4\pi C_p}\left(\frac{1}{LC_p}\right)^{1/2} \tag{14}$$

where $C(d)$ is the blade capacitance as previously denoted in equation (1) and illustrated in figure 3. The blade capacitance is small compared with C_p. After equation (14) is rearranged, $C(d)$ becomes

$$C(d) = -4\pi \Delta f_c C_p \left(LC_p\right)^{1/2} \tag{15}$$

which expresses the basic relationship between the clearance as reflected in $C(d)$ and the quantities Δf_c, L, and C_p.

It is clear from equation (14) that errors in the peak frequency deviation can be introduced by changes in L and C_p. The influence of these effects is discussed as part of the FM oscillator evaluation described in the next few sections.

Calibration and Circuit Measurements

The FM oscillator of figure 4 was calibrated in the static mode at room temperature by using the calibration system of figure 7. The rotor blade tip was 1.2 mm (0.047 in.) thick at its widest point and was 4.0 cm (1.6 in.) long. A precision positioner translated the blade in the direction indicated in the figure. The clearance d was the distance from the blade tip to the probe face.

An oscilloscope and a modulation meter with a 50-Ω input impedance were connected across terminal pair 4-4′ (fig. 4). The oscilloscope showed the oscillator signal output to be of sinusoidal shape with an amplitude of 0.8 V (peak to peak).

Digital displays of frequency and frequency deviation were available on the modulation meter. The frequency display indicated that the oscillator carrier frequency was 42.8 MHz. To compare this measured value of frequency with that calculated from equation (12), the values of L and C_p are required. By using an RF vector impedance meter L and C_p were found to be 0.237 μH and 60.0 pF, respectively. The resultant calculated value of the carrier frequency was 42.2 MHz. The close agreement between these two frequen-

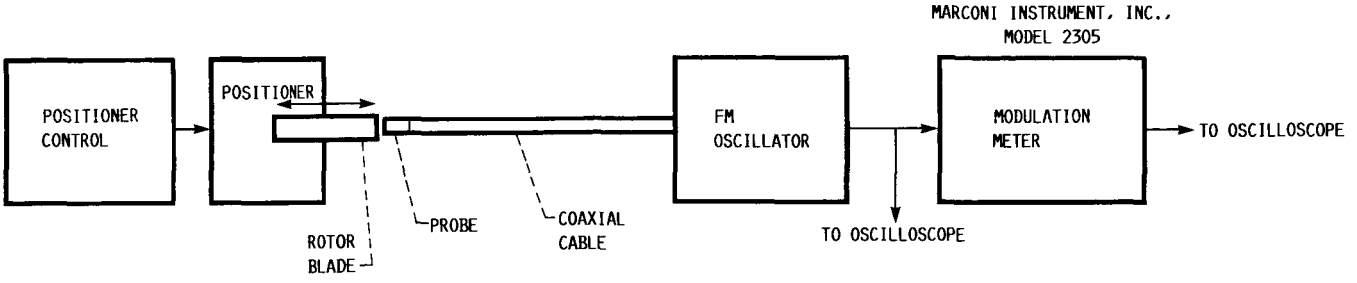

Figure 7.—Block diagram of calibration system.

cies implies that there are no other significant reactances in the equivalent circuit. This verifies the assumption made previously that the reactance at the operational amplifier input can be neglected.

By using the RF vector impedance meter the inductor's effective series resistance R was measured to be approximately 1 Ω. This gave the inductor a Q of approximately 60.

In addition to the digital displays the modulation meter had a filtered analog output signal corresponding to the instantaneous value of frequency deviation. As was stated in the Introduction, the modulating signals may have frequency components up to 1 MHz. The widest bandpass filter available on the meter covers the "flat" range from 10 to 300 kHz, which is somewhat narrower than the desired frequency response. The oscilloscope display of the analog output signal for this filter (fig. 8) shows residual FM oscillator noise of approximately 1.2 kHz (peak to peak). It was estimated that the residual FM oscillator noise for the full 1-MHz bandpass would be approximately 2 kHz (peak to peak) or ±1 kHz (peak). This is the minimum level of detectability for frequency deviation measurements. The influence of this level of noise on the clearance error is discussed in the section "High-Temperature Evaluation and Shunt Capacitance Error Correction."

For the given probe size and blade thickness the negative peak frequency deviation at 1-μm (0.04-mil) clearance (fig. 9) was approximately 400 kHz, and the clearance range was approximately 1000 μm (0.04 in.).

The blade capacitance $C(d)$ was calculated from the

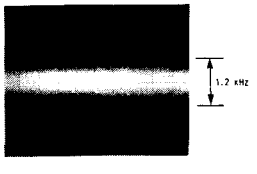

Figure 8.—Analog output of modulation meter showing residual FM oscillator noise. (Vertical scale, 0.5-kHz deviation/division; horizontal scale, 0.1 msec/division).

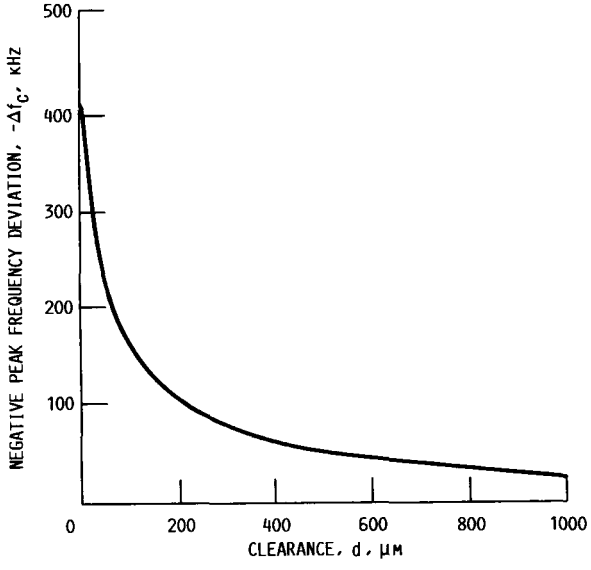

Figure 9.—Calibration curve.

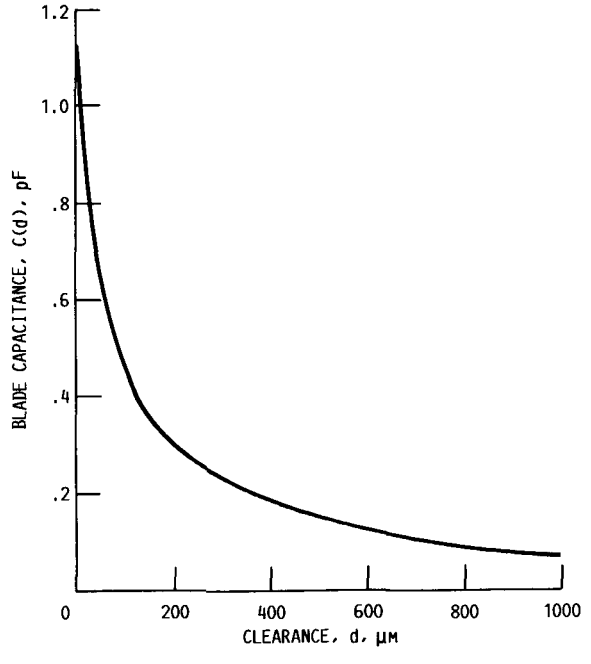

Figure 10.—Blade capacitance as function of clearance.

calibration data and the measured values of L and C_p by using equation (15). The blade capacitance at 1-μm (0.04-mil) clearance. (fig. 10) was approximately 1.2 pF.

Environmental Effects

Errors can be introduced when attempting to use the calibration curve (fig. 9) under conditions different from the calibration environment. The important environmental sources of error are temperature, humidity, vibration, and engine-generated contamination. One or more of these conditions may cause changes in all of the network elements of figure 6(b).

The equivalent shunt capacitance C_p is influenced by temperature, humidity, and engine contamination. The effect of temperature-related changes in C_p as a source of error is discussed in the next two sections. Variations in C_p caused by changes in humidity and engine contamination were not investigated. However, an automatic frequency control method that compensates for environmentally induced changes in C_p is proposed in the section "High-Temperature Evaluation and Shunt Capacitance Error Correction."

The inductance L is influenced primarily by temperature. Its effect on the error in frequency deviation is discussed in the next sections.

Environmental conditions may affect the signal level of the oscillator. Changes in the passive elements of equation (9) cause adjustments in the active element to maintain equilibrium. Like C_p, the value of R_p is influenced by temperature, humidity, and engine contamination. As pointed out in appendix B, an adequate signal level can be maintained, however, if the added shunt resistance does not fall below 10 kΩ.

Vibration may introduce noise and instability to the measurement system. The effect would be most noticeable at low frequencies, where the vibration amplitudes are the largest. If the electronics unit is properly isolated and the probe is rigidly mounted, only the connecting coaxial cable is free to vibrate. To assess this effect, the cable was mounted to an electrodynamic shaker and subjected to a sine wave vibration of 1.6-mm (0.063-in.) peak-to-peak amplitude at frequencies up to 50 Hz. With the FM oscillator connected in the calibration configuration the analog output of the modulation meter was monitored during vibration. No change in the signal was detected, indicating that cable vibration at the level used in this test does not introduce errors in frequency deviation.

Error Analysis of Shunt Capacitance and Inductance

As has been pointed out, errors can be introduced by environmentally induced effects in C_p and L. In this section an expression is derived for the error in peak frequency deviation as a function of the frequency deviations caused by changes in C_p and L.

Let a change in environment cause a small change in the peak frequency deviation denoted by $\delta(\Delta f_c)$. From equation (14) the fractional error can be expressed as

$$\frac{\delta(\Delta f_c)}{\Delta f_c} = -\frac{3}{2}\frac{\delta C_p}{C_p}\bigg|_{L \text{ constant}} - \frac{1}{2}\frac{\delta L}{L}\bigg|_{C_p \text{ constant}} \tag{16}$$

where δC_p and δL are the small changes in C_p and L, respectively, caused by the environmental changes. Thus the fractional error in Δf_c is the weighted sum of the fractional changes in C_p and L.

The two factors in equation (16) are not determined directly but are measured in terms of the frequency deviation caused by their respective parameter changes. From equation (12)

$$\frac{\delta f_c}{f_c}\bigg|_{C_p \text{ constant}} = -\frac{1}{2}\frac{\delta L}{L}\bigg|_{C_p \text{ constant}} \tag{17}$$

$$\frac{\delta f_c}{f_c}\bigg|_{L \text{ constant}} = -\frac{1}{2}\frac{\delta C_p}{C_p}\bigg|_{L \text{ constant}} \tag{18}$$

where δf_c is the frequency deviation due to environmental effects. By substituting equations (17) and (18) into equation (16), it can be written as

$$\frac{\delta(\Delta f_c)}{\Delta f_c} = 3\frac{\delta f_c}{f_c}\bigg|_{L \text{ constant}} + \frac{\delta f_c}{f_c}\bigg|_{C_p \text{ constant}} \tag{19}$$

Equation (19) represents the fractional error in the peak frequency deviation as the weighted sum of the fractional change of the frequency deviations caused by the changes in C_p and L. In equations (16) and (19) note that for the same fractional change the error introduced by C_p is three times the error introduced by L. For example, in equation (16) a 1 percent change in C_p introduces a $-3/2$ percent error but the same change in L introduces only a $-1/2$ percent error.

High-Temperature Evaluation and Shunt Capacitance Error Correction

The effect of high temperature on clearance measurement was evaluated under the most severe test conditions consistent with the chosen design and materials. The calibration curve was used to convert errors in peak frequency deviation to errors in clearance. The results are compared here to the minimum level of detectable clearance caused by the presence of residual FM oscillator noise. A compensation method that corrects for C_p error is also discussed in this section.

Because C_p and L are subject to different temperature environments, the factors of equation (19) were evaluated by

conducting separate high-temperature tests and combining the results. To assess C_p, the effects of C_L and C_k were neglected. The probe and approximately 13 cm (5 in.) of the adjacent coaxial cable were heated from room temperature to 600 °C (1110 °F), the maximum permissible seal temperature. This heating resulted in a change of −55 kHz in the carrier frequency, or a −0.13 percent change in f_c.

To assess the effect of L, it would have been necessary to thermally isolate the inductor from the rest of the oscillator electronics circuit. Instead, the complete circuit was heated from room temperature to 60 °C (140 °F), and the entire change in frequency was attributed to L. The change in frequency was −33 kHz, or −0.08 percent change in f_c.

Adding up the absolute values of the weighted errors in equation (19) resulted in a peak frequency deviation error of slightly less than 0.5 percent, 0.4 percent of which was contributed by changes in C_p. This error can be converted to an error in clearance by using the slope of the calibration curve, which is defined as

$$m = \frac{\delta(\Delta f_c)}{\delta d} \tag{20}$$

where δd is the error in d. In terms of the fractional error in the peak frequency deviation the clearance error is

$$\delta d = \left[\frac{\delta(\Delta f_c)}{\Delta f_c}\right] \frac{\Delta f_c}{m} \tag{21}$$

Since the slope of the calibration curve varies with d, the error is also a function of d. The clearance error due to the effects of high temperature (fig. 11) is less than ±3 μm (0.1 mil) at a clearance of 500 μm (20 mil). Solving for δd from equation (20) allowed the minimum level of detectable clearance as a result of the estimated ±1 kHz (peak) of residual FM oscillator noise to be plotted in the figure. This error is ±10 μm (±0.4 mil) at a clearance of 0.50 mm (0.02 mil). Comparing the two curves shows that at larger clearances the clearance error is dominated by the residual FM oscillator noise.

As noted above, 80 percent of the peak frequency deviation error is contributed by the change in C_p. It is proposed that an automatic frequency control method compensate for these changes. Figure 12 shows the network of figure 6(b) with an additional parallel circuit consisting of the series combination of a large bypass capacitor C_a and the element labeled $C_D(V)$. This element is a reverse-biased PN junction diode, often called a varactor, whose capacitance can be varied by the externally applied voltage V. The corrected capacitance is now

$$C_{p,\text{corrected}} = C_p + C_D(V) \tag{22}$$

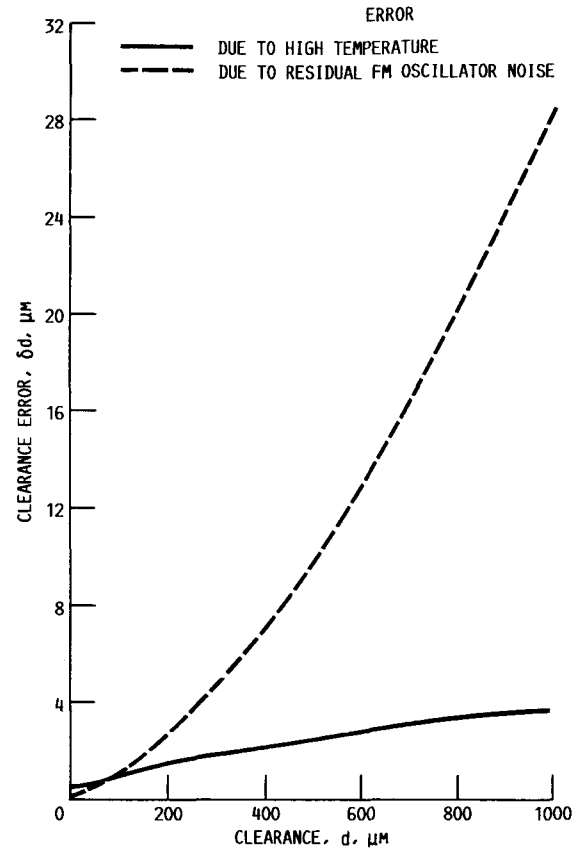

Figure 11.—Clearance errors due to effects of high temperature and residual FM oscillator noise.

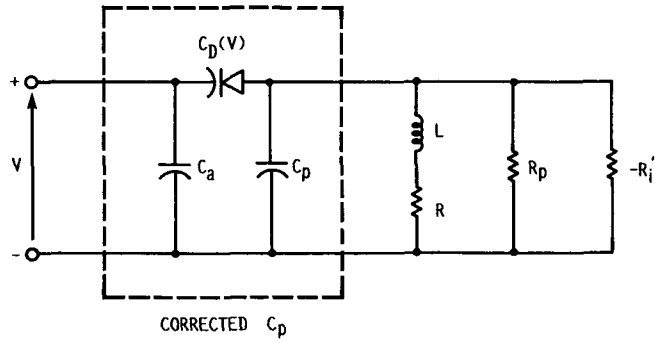

Figure 12.—Equivalent network of figure 6(b) with C_p correction elements.

A feedback loop, not shown, detects the difference between the average oscillator frequency at $C = C_o$ and a reference corrected carrier frequency. The oscillator frequency is measured by sampling the demodulated output signal between blade pairs with an electronic shaft angle encoder (ref. 11) and then filtering. The difference signal generates a voltage that drives $C_D(V)$ in the direction to maintain the oscillator at the corrected carrier frequency and thereby sustain the shunt capacitance at corrected C_p. It is estimated that the oscillator can be controlled to within ±1 kHz of the reference corrected

carrier frequency. Thus the error due to changes in C_p can be reduced from -0.13 percent to less than ± 0.003 percent, a negligibly small value. This technique will not compensate for changes in L.

Concluding Remarks

An FM oscillator consisting of a low-cost operational amplifier circuit and an integrated engine-mounted capacitance probe and coaxial cable has been described. Performance tests showed good accuracy up to a temperature of 600 °C (1110 °F). With further probe design for operation at higher temperatures and the addition of a miniature frequency discriminator, the resultant blade tip clearance measurement system should be applicable to a wide class of fans, compressors, and turbines.

Lewis Research Center
National Aeronautics and Space Administration
Cleveland, Ohio, April 24, 1987

Appendix A
Transmission Line Parameters for Coaxial Cable

In this appendix an equivalent circuit for the coaxial cable based on a short, lightly loaded, nonideal transmission line subject to high temperatures is developed. It is shown that the coaxial cable can be considered to be the parallel combination of a lumped shunt capacitance and a lumped shunt conductance.

Referring to figure 5 let Y_2 be the input admittance of a coaxial cable loaded by Y_1. From transmission line theory (ref. 12), it is known that the input admittance of a loaded transmission line can be written as

$$Y_2 = \frac{1}{Z_0}\left[\frac{Y_1 Z_0 + \tanh \gamma\ell}{1 + Y_1 Z_0 \tanh \gamma\ell}\right] \tag{A1}$$

where Z_0 is the characteristic impedance, γ is the propagation constant, and ℓ is the length of the line. When the electrical length of the line is short (i.e., less than one-fourth of the wavelength at the carrier frequency), then

$$Y_2 = \frac{1}{Z_0}\left\{\frac{Y_1 Z_0 + \gamma\ell - \frac{(\gamma\ell)^3}{3} + \frac{2(\gamma\ell)^5}{15} - \ldots}{1 + Y_1 Z_0\left[\gamma\ell - \frac{(\gamma\ell)^3}{3} + \frac{2(\gamma\ell)^5}{15} - \ldots\right]}\right\} \tag{A2}$$

In order to simplify the following development, only the first term of the series will be retained.

It is also known that

$$\frac{\gamma}{Z_0} = j2\pi f_c c_T + g_T \tag{A3}$$

$$Z_0\gamma = j2\pi f_c l_T + r_T \tag{A4}$$

where c_T, g_T, l_T, and r_T are the distributed shunt capacitance, shunt conductance, series inductance, and series resistance, respectively, of a transmission line. The usual approximation is to neglect the power-absorbing parameters g_T and r_T and call the result an ideal transmission line. At high temperatures, however, these elements cannot be ignored. The shunt conductance is proportional to the conductivity of the ceramic insulator between the inner and outer conductors of the coaxial cable. Since the conductivity of ceramic materials increases with increasing temperature (ref. 13), g_T cannot be neglected. Moreover, the series resistance is proportional to the resistivity of the metal coaxial cable conductors. Since the resistivity of metals increases with increasing temperature, r_T also cannot be ignored. Thus the model of a coaxial cable for high temperatures must include the nonideal transmission line parameters.

Substituting equations (A3) and (A4) into the simplified equation (A2) yields the expression

$$Y_2 = \frac{Y_1 + (j2\pi f_c c_T + g_T)\ell}{1 + Y_1(j2\pi f_c l_T + r_T)\ell} \tag{A5}$$

When the following inequality is met

$$\frac{1}{(j2\pi f_c \ell_T + r_T)\ell} >> Y_1 \qquad \text{(A6)}$$

then

$$Y_2 = Y_1 + (j2\pi f_c c_T + g_T)\ell = Y_1 + j2\pi f_c C_T + G_T \qquad \text{(A7)}$$

where C_T and G_T replace $c_T\ell$ and $g_T\ell$, respectively. The constraint expressed by inequality (A6) limits the application of equation (A7) to a coaxial cable that is lightly loaded (i.e., one whose series admittance is large compared with the admittance of the load Y_1). Since this is the case for the measurement system, the coaxial cable can therefore be considered to be the parallel combination of a lumped shunt capacitance and a lumped shunt conductance.

Appendix B
Amplifier Negative Resistance

Under the proper circumstances the active element nature of an operational amplifier can produce a negative input impedance characteristic. This appendix shows that for the amplifier in the FM oscillator (1) the value of negative resistance is a decreasing function of the amplitude at the input and (2) adequate output signal level is maintained with an added shunt resistance as low as 10 kΩ.

The measurement system for determining the amplifier negative resistance characteristics is shown in figure 13. A coaxial "T" connector is inserted at the junction of the coaxial cable and the oscillator electronics connector (terminal pair 2-2′ in fig. 4). A coaxial resistor of 4.7 kΩ is placed in series with the "T," and a network analyzer measures the voltage transfer function V_B/V_A across the resistor. The value of the resistor is chosen small enough to prevent the circuit from oscillating, thereby permitting the amplifier characteristics to be measured.

Figure 14 is the equivalent network of figure 6(b) with four additional measurement system elements. In addition to the 4.7-kΩ series resistor, C_g is added to simulate the capacitance introduced at the "T" connector. The signal source of the network analyzer is represented by a voltage generator and a 50-Ω resistance.

The presence of C_g causes a shift in the resonant frequency of the circuit. Although this change will result in a somewhat different input characteristic, it is adequate for the purposes of this appendix.

The new resonant frequency was found by tuning the source to the point where the phase of V_B/V_A was equal to zero. Under this condition it can be shown that

$$\frac{R(C_p + C_g)}{L} + \frac{1}{R_p} - \frac{1}{R_i'} = -\frac{1}{4700}\left(1 - \frac{1}{\frac{V_B}{V_A}}\right) = -\frac{1}{R_a} \qquad \text{(B1)}$$

where R_a is an equivalent added shunt resistance. The far left side of equation (B1) is the same as the left side of equations (8) and (9) except for the presence of C_g and the use of C_p instead of C_p'.

The curve of $1/R_a$ is a decreasing function of input amplitude V_B (fig. 15). This is the criterion for the amplitude of oscillation to increase and reach a steady state after initiation by noise.

When R_a is equal to infinity, the output amplitude should be close to the value of the oscillation amplitude (fig. 16). The value of 0.91 V is larger than the oscillation amplitude of 0.80 V, however, because of the presence of C_g. An adequate signal level can be maintained if the added shunt resistance does not fall below an estimated 10 kΩ, the encircled point on the figure.

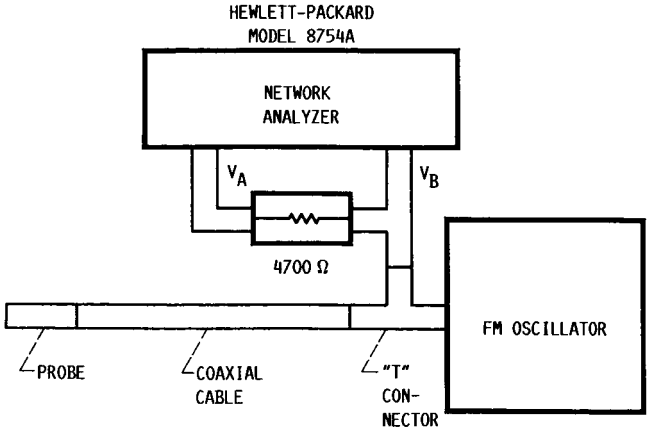

Figure 13.—Measurement system for determining amplifier negative resistance characteristics.

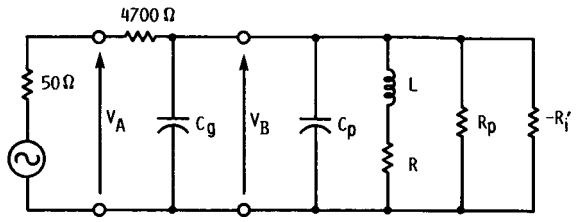

Figure 14.—Equivalent network of figure 6(b) with measurement system elements.

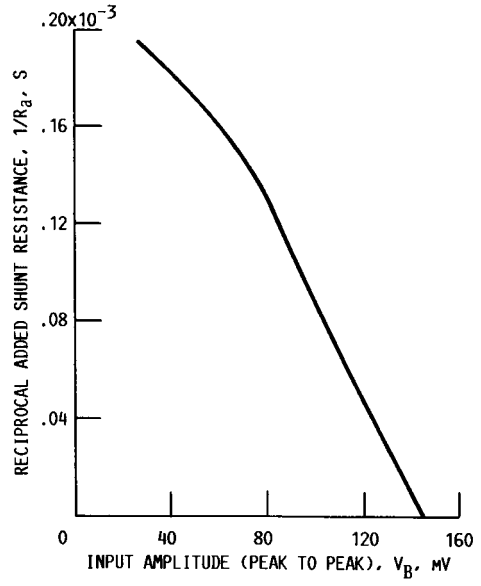

Figure 15.—Reciprocal of added shunt resistance as a function of input amplitude.

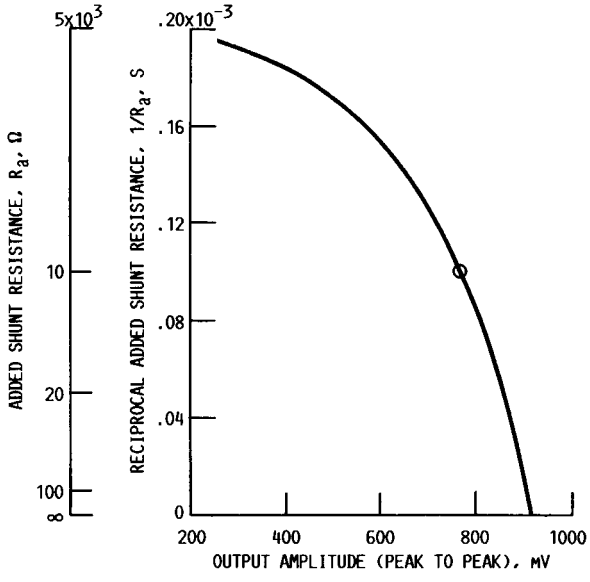

Figure 16.—Added shunt resistance and its reciprocal as functions of output amplitude.

References

1. Barranger, J.P.: In-Place Recalibration Technique Applied to a Capacitance-Type System for Measuring Rotor Blade Tip Clearance. NASA TP-1110, 1978.
2. Doebelin, E.O.: Measurement Systems: Application and Design. McGraw-Hill, 1966, p. 254.
3. Mayer, R.: Apparatus for Measuring Blade-Die in a Pelletizer Including Rotating Capacitor Blade. U.S. Patent 3,428,889, Feb. 18, 1969.
4. Wobschall, D.: Circuit Design for Electronic Instrumentation. McGraw-Hill, 1979, p. 139.
5. Scotto, M.J.; and Eismeier, M.E.: High-Speed Noncontacting Instrumentation for Jet Engine Testing. J. Eng. Power, vol. 102, no. 4, Oct. 1980, pp. 912–917.
6. Demers, R.N.: Compressor Blade Clearance Measurement Using Capacitance and Phase Lock Techniques. Advanced Instrumentation for Aero Engine Components, AGARD CP-399, 1986, pp. 30–1 to 30–10.
7. Knoell, H.; and Ding, K.: Tip Clearance Measurement in Modern Compressor Components. Advanced Instrumentation for Aero Engine Components, AGARD CP-399, 1986, pp. 29–1 to 29–10.
8. Jonas, R.P.: Means for Measuring Clearances in a Gas Turbine Including Coaxial Cable Capacitor. U.S. Patent 3,628,136, Dec. 14, 1971.
9. Paulon, J.: Influence et Mesure du Jeu en Bout D'Aubes dans les Turbomachines (The Effect and Measurement of Blade Tip Clearance in Turbomachinery). Heat Transfer and Cooling in Gas Turbines, AGARD CP-390, 1985, pp. 34–1 to 34–8.
10. Sarma, G.R.; and Barranger, J.P.: Ramp-Integration Technique for Capacitance-Type Blade-Tip Clearance Measurement. NASA TM-87241, 1986.
11. Technical Information Manual, Electronic Shaft Angle Encoder, Model 371. Real Time Systems, Inc., Mount Vernon, N.Y., Sept. 1978.
12. Reference Data for Radio Engineers. Sixth ed., Howard W. Sams & Co., 1975, p. 24–4.
13. Van Vlack, L.H.: Physical Ceramics for Engineers, Addison-Wesley, 1964, p. 173.

NASA
National Aeronautics and Space Administration

Report Documentation Page

1. Report No.	2. Government Accession No.	3. Recipient's Catalog No.
NASA TP-2746		

4. Title and Subtitle	5. Report Date
Low-Cost FM Oscillator for Capacitance Type of Blade Tip Clearance Measurement System	July 1987
	6. Performing Organization Code: 505-62-01

7. Author(s)	8. Performing Organization Report No.
John P. Barranger	E-3455
	10. Work Unit No.

9. Performing Organization Name and Address	11. Contract or Grant No.
National Aeronautics and Space Administration Lewis Research Center Cleveland, Ohio 44135	13. Type of Report and Period Covered: Technical Paper
12. Sponsoring Agency Name and Address	14. Sponsoring Agency Code
National Aeronautics and Space Administration Washington, D.C. 20546	

15. Supplementary Notes

16. Abstract

The frequency-modulated (FM) oscillator described in this report is part of a blade tip clearance measurement system that meets the needs of a wide class of fans, compressors, and turbines. As a result of advancements in the technology of ultra-high-frequency operational amplifiers, the FM oscillator requires only a single low-cost integrated circuit. Its carrier frequency is 42.8 MHz when it is used with an integrated probe and connecting cable assembly consisting of a 0.81-cm (0.32-in.) diameter engine-mounted capacitance probe and a 61-cm (24-in.) long hermetically sealed coaxial cable. A complete circuit analysis is given, including amplifier negative resistance characteristics. An error analysis of environmentally induced effects is also derived, and an error-correcting technique is proposed. The oscillator can be calibrated in the static mode and has a negative peak frequency deviation of 400 kHz for a rotor blade thickness of 1.2 mm (0.047 in.). High-temperature performance tests of the probe and 13 cm (5 in) of the adjacent cable show good accuracy up to 600 °C (1100 °F), the maximum permissible seal temperature. The major source of error is the residual FM oscillator noise, which produces a clearance error of ± 10 μm (± 0.4 mil) at a clearance of 0.5 mm (0.02 in.). The oscillator electronics accommodates the high rotor speeds associated with small engines, the signals from which may have frequency components as high as 1 MHz.

17. Key Words (Suggested by Author(s))	18. Distribution Statement
Tip clearance measurements; Turbomachinery; Instrument standards and calibration techniques; Nondestructive tests; Spacecraft instruments; Aircraft instruments; Sensors; Transducers	Unclassified – unlimited STAR Category 07

19. Security Classif. (of this report)	20. Security Classif. (of this page)	21. No of pages	22. Price*
Unclassified	Unclassified	16	A02

NASA FORM 1626 OCT 86

*For sale by the National Technical Information Service, Springfield, Virginia 22161

NASA-Langley, 1987